https://doi.org/10.5194/egusphere-2026-1574
Preprint. Discussion started: 24 March 2026

Five-channel TD–CEAS measurements of gaseous and particulate organic nitrates with NO/NO_2 interference correction under high-NO_x conditions

Xiao Tian [1, 2], Hongcheng Lu [1, 3], Wei Song [1, *], Xue Yu [1, 2], Xinming Wang [1, 2, *]

[1] State Key Laboratory of Advanced Environmental Technology and Guangdong Key Laboratory of Environmental Protection and Resources Utilization, Guangzhou Institute of Geochemistry, Chinese Academy of Sciences, Guangzhou 510640, China

[2] College of Resources and Environment, University of Chinese Academy of Sciences, Beijing 100049, China

[3] School of Earth and Space Sciences, University of Science and Technology of China, Hefei 230026, China

*Correspondence: Wei Song (songw@gig.ac.cn); Xinming Wang (wangxm@gig.ac.cn)

https://doi.org/10.5194/egusphere-2026-1574
Preprint. Discussion started: 24 March 2026

Abstract

Organic nitrates (ONs) are important temporary reservoirs of atmospheric NOx and, for sufficiently low-volatility species, contributors to secondary organic aerosol formation. However, online measurements of particle-phase ONs remain limited, hindering quantitative constraints on ON abundance and gas–particle partitioning. Here we present a five-channel thermal dissociation cavity-enhanced absorption spectrometer (TD–CEAS) for in situ, time-resolved measurements of NO_2 and operationally defined ON classes in both the gas and particle phases. The instrument combines a room-temperature channel for ambient NO_2 with thermal dissociation channels operated at 250 and 450 °C to quantify total peroxy nitrates (ΣPNs) and total alkyl nitrates (ΣANs), respectively. Gas–particle separation is achieved using paired inlet/filter configurations, and gas- and particle-phase ΣPNs and ΣANs are retrieved by channel differencing. The 1σ (1 s) detection limits are 49 pptv for gΣPNs, 49 pptv for pΣPNs, 48 pptv for gΣANs, and 68 pptv for pΣANs. Laboratory characterization included temperature-dependent dissociation measurements, cross-validation of PAN against GC–ECD (R^2=0.988; slope = 0.987), and an operational calibration for particulate ΣANs using 2-ethylhexyl nitrate (recovery slope=1.036±0.028; method detection limit =0.029 μg NO_2). Dedicated interference experiments showed that NO and NO_2 can introduce substantial nonlinear biases in ΣPN measurements; these effects were parameterized using a multiple nonlinear regression model. The instrument was deployed at an urban site in Guangzhou during September–October 2025 and provided 6 min measurements of NO_2, gas- and particle-phase ΣPNs, and gas- and particle-phase ΣANs under high-NOx conditions. During the October intensive period, corrected gas-phase ΣPNs covaried well with independently measured PAN (R^2=0.83), and PAN accounted for 78 % of daytime gΣPNs. This five-channel TD–CEAS provides a framework for continuous observations of ON phase partitioning and reactive nitrogen processing in polluted urban atmospheres.

Keywords: thermal dissociation; cavity-enhanced absorption spectroscopy; NO_2; peroxy nitrates; alkyl nitrates; gas–particle partitioning

https://doi.org/10.5194/egusphere-2026-1574
Preprint. Discussion started: 24 March 2026

1 Introduction

Organic nitrates (ONs), defined here as organic compounds containing the $–ONO_2$ functional group, are ubiquitous in the atmosphere. They are produced primarily during the oxidation of volatile organic compounds (VOCs) in the presence of NOx via daytime OH chemistry and nighttime NO_3 chemistry. By temporarily sequestering NOx and subsequently releasing it through thermal decomposition, photolysis, and further oxidation (Kirchner et al., 1999; Neu et al., 2008), ONs act as both reservoirs and sinks of reactive nitrogen, thereby influencing ozone production and the redistribution of NOx on regional scales (Perring et al., 2013). In addition, many ONs are sufficiently low in volatility, or become so through continued oxidation and accretion, that they partition to the particle phase and contribute to secondary organic aerosol (SOA) formation (Atkinson, 2000; Rollins et al., 2012). Quantifying ON abundance and gas-particle partitioning is therefore important for constraining both reactive nitrogen budgets and coupled oxidant–aerosol chemistry.

Operationally, ONs are often grouped into peroxy nitrates (RO_2NO_2, ΣPNs) and alkyl nitrates ($RONO_2$, ΣANs), which differ in formation pathways, thermal stability, and atmospheric lifetimes (Roberts, 1990). Acyl peroxy nitrates such as peroxyacetyl nitrate (PAN) and peroxypropionyl nitrate (PPN) are relatively thermally stable and can represent a substantial fraction of ΣPNs, whereas non-acyl peroxy nitrates such as HO_2NO_2 and $CH_3O_2NO_2$ are much less stable under typical boundary-layer conditions (Murphy et al., 2004). ΣANs are produced in both OH- and NO_3-initiated oxidation, with especially important contributions from nighttime NO_3 chemistry and implications for SOA formation and reactive nitrogen cycling (Rollins et al., 2012; Perring et al., 2013). The structural diversity, multifunctionality, and composition-dependent

https://doi.org/10.5194/egusphere-2026-1574
Preprint. Discussion started: 24 March 2026

volatility of ONs make them challenging targets for comprehensive, in situ measurements, particularly when both gas- and particle-phase ONs are of interest.

Thermal dissociation (TD) coupled with fast NO_2 detection has emerged as a practical approach for class-resolved ON measurements because the O–NO_2 bond strengths differ between RO_2NO_2 and $RONO_2$, enabling ΣPNs and ΣANs to be converted to NO_2 at different temperatures (Roberts, 1990; Kirchner et al., 1999). TD has been combined with a range of sensitive NO_2 detectors, including laser-induced fluorescence (LIF) (Day et al., 2002), cavity ring-down spectrometry (CRDS) (Paul et al., 2009), chemical ionization mass spectrometry (CIMS) (Zheng et al., 2011), cavity attenuated phase shift spectrometry (CAPS) (Sadanaga et al., 2016), and cavity-enhanced absorption spectrometry (CEAS) (Li et al., 2021). These instruments have enabled sensitive measurements of gas-phase ON classes, and recent work has also extended TD-based approaches to the particle phase (Keehan et al., 2020). Nevertheless, online measurements of particle-phase ONs remain comparatively limited. In many studies, particle-phase ONs are inferred indirectly from aerosol mass spectrometry or derived from offline filter analysis, both of which have limitations in chemical specificity, time resolution, or operational simplicity (Yu et al., 2019; Chen et al., 2022). Extending TD-based measurements to particle-phase ONs requires careful inlet design, phase separation, and evaluation of potential sampling artifacts.

A central challenge in TD-based ΣPN measurements is that thermal dissociation does not simply convert the analyte to NO_2; it also produces radical intermediates that can participate in secondary chemistry within the heated inlet. In particular, dissociation of peroxy nitrates yields RO_2 radicals, which can react with NO to form additional NO_2, biasing ΣPNs high, or recombine with NO_2 to re-form peroxy nitrates, biasing ΣPNs

https://doi.org/10.5194/egusphere-2026-1574
Preprint. Discussion started: 24 March 2026

low (Day et al., 2002; Li et al., 2021; Lin et al., 2024). The direction and magnitude of the bias depend on the chemical regime in the inlet and are therefore expected to be especially important under high-NOx conditions, where NO and NO_2 coexist at elevated concentrations and vary rapidly. This issue is not merely a calibration detail: for TD instruments deployed in polluted urban air, inaccurate treatment of NO/NO_2-dependent chemistry can directly compromise the quantitative retrieval of ΣPNs.

Several strategies have been proposed to reduce or correct these interferences. Hardware-based approaches include decreasing the residence time available for secondary chemistry by modifying inlet pressure or flow conditions (Day et al., 2002), adding downstream packing materials intended to remove radical intermediates (Lin et al., 2024), or redesigning the dissociation channel and introducing O_3 downstream so that NO is converted to NO_2 and the instrument effectively measures NOx rather than NO_2 alone (Wüst et al., 2025). Calibration-based approaches have also been used, in which known NO or NO_2 perturbations are applied to PAN standard gas and the resulting deviations are represented as correction factors or lookup tables for ambient data processing (Li et al., 2021). These approaches have improved TD measurements substantially, but they also have limitations. In ambient air, NO and NO_2 generally vary simultaneously rather than independently, and the relative importance of the competing pathways is governed by the chemical regime rather than by either species alone. In addition, PAN standards are commonly generated photochemically from acetone-containing systems, which may introduce excess peroxyacetyl radicals and other secondary products that complicate the interpretation of separate NO and NO_2 addition experiments. Under high-NOx conditions, where both interferences may occur simultaneously, treating NO and NO_2 effects independently may therefore be insufficient.

https://doi.org/10.5194/egusphere-2026-1574
Preprint. Discussion started: 24 March 2026

These considerations are particularly important for multi-channel instruments designed to retrieve both gas- and particle-phase ΣPNs and ΣANs. In such systems, a bias in the ΣPN channel propagates directly into the derived gas-phase signal and can also affect the particle-phase product through channel differencing. A robust treatment of NO/NO_2 -dependent interference is therefore essential not only for accurate ΣPN quantification, but also for reliable gas-particle partitioning in polluted environments. At the same time, there remains a practical need for compact instruments that can measure ON classes in both phases using a single NO_2 detector and a field-deployable inlet architecture.

In this work, we develop a five-channel thermal dissociation TD-CEAS that extends TD-CEAS for in situ measurements of gaseous and particulate ONs. The instrument combines a single CEAS NO_2 detector with two TD setpoints (250 °C for ΣPNs and 450 °C for ΣANs) and paired filter configurations to retrieve gas- and particle-phase ΣPNs and ΣANs by channel differencing. Particular emphasis is placed on the characterization and correction of NO/NO_2-dependent interference in the ΣPN channels under high-NOx conditions. To this end, we perform dedicated laboratory experiments, develop a multiple nonlinear regression correction model for the combined effects of NO and NO_2, and compare its performance with a previously reported lookup-table approach. We further characterize the instrument response, evaluate its precision and detection limits, and demonstrate its performance during an urban field deployment in Guangzhou. This study aims to provide both a practical measurement framework for continuous ON observations in gas and particle phases and a correction strategy for improving TD-based ΣPN measurements in chemically complex, high-NOx environments, enabling derivation of gas- and particle-phase ON classes by channel differencing. We provide systematic laboratory characterization, including dissociation

https://doi.org/10.5194/egusphere-2026-1574
Preprint. Discussion started: 24 March 2026

behavior, calibration strategies for gaseous and particulate standards, and quantification of interferences relevant to high-NOx environments, and we demonstrate the instrument performance during an urban field deployment.

2 Instrumentation and methods

2.1 Thermal dissociation (TD) inlets

TD is implemented using heated quartz-tube reactors. Each TD inlet consists of a quartz tube (60 cm length; 1/4″ outer diameter; 3.9 mm inner diameter) wrapped with 20 cm Ni–Cr heating wire and insulated with thermal cotton to minimize heat loss. A K-type thermocouple positioned at the center of the heated region monitors the tube outer-wall temperature and is regulated by a temperature controller (stability ±2 °C). The thermocouple accuracy is ± 1 °C over -20–1000 °C.

Sample air is delivered through 1/4″ PTFE tubing with PTFE straight/tee fittings (Swagelok). During operation, the sampling flow is 1 L min^{-1}, corresponding to a residence time of 0.048 s in the heated region. This short residence time is designed to promote rapid dissociation of thermally labile ONs while minimizing post-dissociation chemistry within the heated section. Because the thermocouple measures the tube wall temperature rather than the gas temperature, the reported TD setpoints are expected to be higher than the corresponding gas temperature. Therefore, TD setpoints reported here should be interpreted as operational setpoints for this specific reactor design and are not necessarily directly comparable with other TD geometries.

2.2 CEAS NO_2 spectrometer

Thermally generated NO_2 is detected by CEAS near 405 nm. In CEAS, an optical cavity provides a long effective absorption pathlength through multiple reflections between high-reflectivity mirrors, enabling sensitive absorption-based NO_2 measurements while retaining the selectivity of optical spectroscopy. NO_2 has strong, structured absorption

https://doi.org/10.5194/egusphere-2026-1574
Preprint. Discussion started: 24 March 2026

in the 405 nm region, allowing retrieval via spectral fitting. A single CEAS NO_2 spectrometer is used for all five inlet channels. The CEAS instrument used here has been characterized previously (Zhou et al., 2022). In the present configuration, the CEAS reports NO_2 mixing ratios for each channel segment, and all TD-derived quantities are obtained by differencing of channel measurements (Sect. 2.5).

2.3 Standards and laboratory generation

2.3.1 PAN (representative ΣPNs)

PAN is used as a representative PN for laboratory characterization of the ΣPN channel. PAN is produced photochemically by UV photolysis (285 nm) of excess acetone in O_2 to generate peroxyacetyl (PA) radicals, followed by reaction with NO (He et al., 2023). PAN mixing ratios are adjusted by varying the NO flow. PAN is quantified independently using a GC-ECD and is used for cross-validation of the TD-CEAS response.

2.3.2 Alkyl nitrates (representative ΣANs) and aerosol tests

Isobutyl nitrate and isopropyl nitrate (95% purity, Macklin, China) are used as representative gas-phase AN for characterization of the ΣAN response. These standards are generated by dilution of their vapor into zero air following established approaches (Paul et al., 2009).

For particle-phase tests, 2-ethylhexyl nitrate (2-EHN, Aladdin, China) solution is aerosolized to produce organic nitrate-containing particles, which are introduced into the TD-CEAS to evaluate particle-phase response and quantification. Because particulate inorganic nitrate may also generate NO_2 upon heating, sodium nitrate aerosol is generated in a similar manner to characterize its temperature-dependent contribution and assess potential interference in the particle-phase channels.

2.4 Five-channel configuration, sampling sequence, and channel definitions

https://doi.org/10.5194/egusphere-2026-1574
Preprint. Discussion started: 24 March 2026

The five-channel TD-CEAS combines two TD temperatures (250 °C and 450 °C) with two filter placements (upstream versus downstream) to enable separation of gas and particle phases (Figure S1). Ambient air is sampled through a $PM_{2.5}$ cyclone prior to entering the inlet manifold. A multi-channel inlet selection unit sequentially routes each channel to the shared CEAS detector.

The instrument samples five channels plus an ultra-high-purity N_2 reference segment. Each channel is sampled for 1 min, followed by a 1 min N_2 segment, yielding a 6-min measurement cycle. The N_2 segment is used as a reference for instrument baseline and stability (Sect. 2.6).

We denote "F" as a particle filter placed upstream of the TD (gas-only enters TD), and "UF" as an inlet without an upstream filter (gas + particle enter TD), with a particle filter placed downstream of the TD reactor to prevent particles from entering the CEAS cavity. Table 1 summarizes the channel definitions and the corresponding quantities measured as NO_2 mixing ratios by CEAS.

2.5 Retrieval of g/p ΣPNs and g/p ΣANs

For each 1 min segment, the CEAS reports an NO_2 mixing ratio for the selected channel. Let $\boldsymbol{C}_{\mathrm{RTF}}$, $\boldsymbol{C}_{250\mathrm{F}}$, $\boldsymbol{C}_{450\mathrm{F}}$, $\boldsymbol{C}_{250\mathrm{UF}}$, and $\boldsymbol{C}_{450\mathrm{UF}}$ denote the NO_2 mixing ratios (pptv or ppbv) measured by CEAS in the corresponding channels. Gas- and particle-phase ON classes are retrieved by channel differencing:

$$g\Sigma PNs = C_{250F} - C_{RTF} \quad (1)$$

$$p\Sigma PNs = C_{250UF} - C_{250F} \quad (2)$$

$$g\Sigma ANs = C_{450F} - C_{250F} \quad (3)$$

$$p\Sigma ANs = (C_{450UF} - C_{250UF}) - (C_{450F} - C_{250F}) \quad (4)$$

https://doi.org/10.5194/egusphere-2026-1574
Preprint. Discussion started: 24 March 2026

These expressions correspond to the field configuration in which the RT/250/450 channels are operated with upstream particle filtration for gas-phase retrieval, while paired 250/450 channels without upstream filtration (but with downstream particle removal) provide total (gas + particle) ON classes.

Because channels are sampled sequentially, each derived quantity is timestamped at the midpoint of the corresponding 1-min segment. When longer averaging periods are applied (e.g., hourly means), within-cycle timing offsets are typically small compared with the averaging window.

2.6 Uncertainty propagation, detection limits, and reporting conventions

Detection limits are reported as 1σ precision inferred from Allan deviation analyses with ultra-high purity N_2 continuously introduced to each channel. For the RT, 250 °C, and 450 °C channels, the 1σ NO_2 detection limits at 1 s integration are 34, 35, and 33 pptv, respectively; at 10 s integration they are 12, 13, and 12 pptv.

Derived ON quantities are calculated as differences between channels. Assuming independent noise among channel measurements, the uncertainty for a difference ***A-B*** is propagated as:

$$\sigma_{A-B} = \sqrt{\sigma_A^2 + \sigma_B^2} \quad (5)$$

Using the 1 s NO_2 precision for relevant channels, the resulting 1σ (1 s) detection limits for derived gas-phase ΣPNs and ΣANs are:

$$\sigma(g\Sigma PNs) = \sqrt{\sigma_{250F}^2 + \sigma_{RTF}^2} \approx \sqrt{35^2 + 34^2} = 49\ pptv \quad (6)$$

$$\sigma(g\Sigma ANs) = \sqrt{\sigma_{450F}^2 + \sigma_{250F}^2} \approx \sqrt{33^2 + 35^2} = 48\ pptv \quad (7)$$

And for particle-phase ONs are:

https://doi.org/10.5194/egusphere-2026-1574
Preprint. Discussion started: 24 March 2026

$$\sigma(p\Sigma PNs) = \sqrt{\sigma_{250UF}^2 + \sigma_{250F}^2} \approx 49\ pptv \quad (8)$$

$$\sigma(p\Sigma ANs) = \sqrt{\sigma_{450UF}^2 + \sigma_{250UF}^2 + \sigma_{450F}^2 + \sigma_{250F}^2} \approx 68\ pptv \quad (9)$$

These values correspond to the reported field-operation performance. Table 2 compares the detection limits of the present TD–CEAS with those reported for representative TD-based techniques. Overall, the detection limits achieved here are within the range of recent TD instruments, while the present configuration additionally enables sequential retrieval of gas- and particle-phase PNs and ANs using a single NO_2 spectrometer. Because published detection limits are reported at different integration times and for different instrument configurations, the comparison is intended as a general benchmark rather than a strict ranking of sensitivity.

2.7 Box model

A zero-dimensional box model was implemented to reproduce the correction-factor lookup table reported by (Li et al., 2021) and to compare that approach with the regression-based correction proposed in this study. The chemical mechanism followed previous work and was based on the Master Chemical Mechanism (MCM) v3.3. The wall loss rate constants for RO_2, HO_2, and OH radicals were set to 0.3, 0.5 and 5.4 s^{-1}, respectively, following Fuchs et al. (2008), Wooldridge et al. (2010), Thieser et al. (2016), and Li et al. (2021). The model was used only for method comparison and not for interpretation of ambient observations.

3 Laboratory characterization

3.1 TD temperature selection and dissociation behavior

To define operational TD temperature for ΣPNs and ΣANs, we measured temperature-dependent NO_2 yields (“thermal spectra”) for representative organic nitrates. PAN was

https://doi.org/10.5194/egusphere-2026-1574
Preprint. Discussion started: 24 March 2026

used as a surrogate acyl peroxy nitrate, isopropyl nitrate and isobutyl nitrate were used as surrogate alkyl nitrates, and 2-ethylhexyl nitrate (2-EHN) aerosol was used as a surrogate particulate organic nitrate. Sodium nitrate aerosol was used to evaluate potential interference from particulate inorganic nitrate.

For each compound, the TD setpoint was stepped across the temperature range and the NO_2 enhancement in the heated channel (relative to room temperature) was used to infer dissociation completeness. As shown in Figure 1, PAN reaches a stable plateau in NO_2 yield at temperatures above ~250 °C, indicating near-complete conversion at and above this temperature. In contrast, isopropyl nitrate and isobutyl nitrate show minimal dissociation below 250 °C (<10% of the high-temperature plateau), increase sharply near ~300 °C, and reach stable plateau by ~350 °C. The particulate 2-EHN shows a similar trend, stabilizing near ~400 °C. Particulate inorganic nitrate behaves differently: the NO_2 yield remains <10% below 400 °C and does not reach a stable plateau until ~750 °C, implying that particulate inorganic nitrate contributes minimally to the NO_2 signal at 450 °C for this TD geometry and residence time.

Based on these measured thermal spectra, we selected 250 °C as the operational setpoint for ΣPNs and 450 °C as the operational setpoint for ΣANs. These setpoints are specific to the present TD reactor design (Sect. 2.1) and correspond to wall temperatures measured at the tube exterior.

3.2 Calibration and quantitative performance

3.2.1 PAN calibration and GC-ECD cross-validation

PAN was generated using the photochemical source described in Sect. 2.3.1 and quantified independently by GC–ECD (Zhang et al., 2012). Over 0–20 ppb supplied NO, the relationship between NO input and generated PAN indicates stable PAN production with an average conversion efficiency of ~84% (R^2 = 0.99). PAN derived

https://doi.org/10.5194/egusphere-2026-1574
Preprint. Discussion started: 24 March 2026

from the TD–CEAS channel agrees closely with GC-ECD across trace to heavily polluted levels (R^2 = 0.988; slope = 0.987; Fig. 2). This agreement supports quantitative retrieval of ΣPNs for representative acyl peroxy nitrates under the tested conditions.

3.2.2 Particle-phase ΣAN calibration via filter thermolysis of 2-EHN

Stable gas-phase ΣAN standards at specified mixing ratios are difficult to generate reproducibly by vapor dilution. Therefore, we established an operational particulate ΣAN calibration using filter thermolysis of 2-EHN (Yu et al., 2021). A known volume of 2-EHN solution was injected onto a pre-baked quartz filter (0.5 cm^2; baked at 450 °C for 4 h) placed inside a quartz TD tube held at 450 °C. A second 450 °C TD stage was installed downstream to promote complete conversion prior to NO_2 detection. The resulting NO_2 signal was measured by CEAS in dry, clean air.

The recovered NO_2 mass from each injection was calculated by integrating the NO_2 time series:

$$m_{NO_2}(\mu g) = \frac{M_{NO_2} Q}{V_m * 10^6} \sum_i ([NO_2]_i \, \Delta t) \quad (10)$$

where $[NO_2]_i$ is the NO_2 mixing ratio in ppb at time step ***i***, M_{NO2} is the molar mass of NO_2 (g mol^{-1}), Q is the CEAS sampling flow (16.67 mL s^{-1}), Δt = 1 s, and V_m = 24.5 L mol^{-1} at 25 °C and 101 kPa. The 10^6 factor converts ppbv and flow units to mass in µg.

Seven blank-filter runs were used to determine method detection limit of 0.029 µg NO_2. 2-EHN calibration using five injection volumes (1, 2, 5, 8, 10 µL) shows excellent linearity (R^2 = 0.99; Fig. 3). The recovery regression slope is 1.036 ± 0.028 with a small intercept (−0.020 ± 0.046), indicating quantitative recovery for this surrogate particulate ΣAN standard under the calibration conditions.

https://doi.org/10.5194/egusphere-2026-1574
Preprint. Discussion started: 24 March 2026

3.3 Interferences and correction strategies

3.3.1 NO and NO_2 interferences on ΣPNs

Thermal dissociation of ΣPNs produces RO_2 radicals that can participate in rapid secondary chemistry within the heated inlet. In the presence of NO_2, these radicals can recombine to re-form peroxy nitrates and bias ΣPNs low. In the presence of NO, they can convert NO to NO_2 and bias ΣPNs high (Day et al., 2002; Sobanski et al., 2016; Li et al., 2021; Lin et al., 2024). These competing pathways are expected to be especially important under high-NOx conditions, where NO and NO_2 coexist at elevated concentrations and vary simultaneously.

To characterize these effects for the present TD geometry, we conducted laboratory interference experiments using PAN as a representative acyl peroxy species. As described in Text S1, PAN was generated photochemically in an acetone/air system while the NO input was progressively increased. PAN was measured by GC-ECD, NO and NO_2 was measured by a Thermo Scientific 42i-TL analyzer, and ΣPNs and ΣANs were measured by TD-CEAS. This configuration enabled direct comparison between the reference PAN concentration and the uncorrected TD-CEAS ΣPNs signal over a range of NO/NO_2 regimes.

During the gradient experiments, the acetone concentration was held constant and only the NO input was varied. At acetone-rich, low-NO conditions, most added NO was converted to NO_2, which promoted PAN formation. Under these conditions, the measured ΣPN signal was biased low because of excess peroxyacetyl (PA) radicals, together with PA radicals produced by PAN dissociation in the TD inlet, could recombine with NO_2 downstream of the heated section. As the NO mixing ratio increased, PAN formation was increasingly suppressed, while PA radicals generated by PAN dissociation reacted increasingly with NO to form additional NO_2, causing the

https://doi.org/10.5194/egusphere-2026-1574
Preprint. Discussion started: 24 March 2026

measured ΣPNs signal to become biased high. These experiments therefore show that both the sign and the magnitude of the bias are governed by the chemical regime in the inlet rather than by NO or NO_2 alone.

To account for the combined effects of NO and NO_2, we developed a multiple nonlinear regression model based on the experimental dataset. Because temperature was held constant in these experiments and PAN formation and dissociation are closely related to the NO/NO_2 ratio (Zhang et al., 2015), the NO/NO_2 ratio was used as the explanatory variable to represent the relevant chemical regime:

$$[\Sigma PNs]_{real} = a \times [\Sigma PNs]_{meas} \times e^{\left(b \times \frac{[NO]}{[NO_2]}\right)} + c \quad (11)$$

where $[\mathbf{\Sigma PNs}]_{real}$ is the PAN reference concentration measured by GC-ECD, $[\mathbf{\Sigma PNs}]_{meas}$ is the uncorrected TD-CEAS concentration, and [NO] and $[NO_2]$ are expressed in ppbv. The ***a***, ***b***, and ***c*** are the fitting coefficients, with values of 1.57, -3.44, and 0.58 respectively.

For comparison, we also reproduced the correction-factor lookup-table correction approach of Li et al. (2021) using the box model configuration described in Sect. 2.7. Figure 4 compares corrected ΣPNs values obtained with the two approaches against the reference PAN measurements with GC-ECD. The multiple nonlinear regression model reproduced the reference PAN vales well (R^2= 0.993; RMSE = 0.49 ppbv) across both low and high PAN ranges. By comparison, the reproduced lookup-table approach performed well at low concentrations (R^2=0.975) but increasing overestimated PAN at high concentrations, particularly under high-NO_x conditions. The corresponding evaluation metrics for both methods are summarized in Table S1. Relative to the lookup-table method, the regression model provides a more compact correction

https://doi.org/10.5194/egusphere-2026-1574
Preprint. Discussion started: 24 March 2026

framework and better captures the coupled effects of NO and NO_2 across the experimental range.

To further assess robustness, replicate experiments were performed under otherwise identical conditions but with different NO gradients. As shown in Fig. S4, the corrected ΣPNs agreed well with the measured PAN, with correlation coefficient of 0.98 and slopes of 1.06, indicating that the regression-based correction was reproducible across independent gradient experiments.

Previous studies have reported the presence of alkyl nitrates in photochemical PAN sources (Paul et al., 2009), consistent with the ΣANs signal observed in the 450 °C channel during these experiments (Fig. S3). However, the ΣANs signal varied only weakly with the NO and NO_2 perturbations. Because NO/NO_2-induced deviations are present in both the 250°C and 450°C channels, and largely cancel in the 450-250 channel subtraction, no additional correction was applied to ΣANs in this study. During field observations, the correction model was applied to the 250 °C channel measurements using simultaneously measured NO and NO_2, and the corrected 250 °C data were then used to derive ΣPNs. Unlike approaches that require downstream ozone addition (Wüst et al., 2025), this method relies only on measured NO and NO_2 and can therefore be implemented directly during field deployment.

3.3.2 O_3 interference

O_3 thermally dissociate at elevated temperatures (>330 °C), producing O atoms that can perturb the NO/NO_2 partitioning in the heated region. Prior laboratory studies indicate that even high O_3 (200–240 ppb) mixed with 25.1 ppb NO_2 results in only ~3.5% NO_2 loss at 600 °C, and no significant NO_2 bias is observed across typical O_3 levels in comparable TD systems (Day et al., 2002). Kinetic estimates under representative

https://doi.org/10.5194/egusphere-2026-1574
Preprint. Discussion started: 24 March 2026

polluted conditions (e.g., O_3 100 ppb, NO 2 ppb, NO_2 5 ppb) suggest that O_3-related NO_2 perturbations in heated channels are within ~3%, smaller than the overall measurement uncertainty. The experiment further demonstrated that variations in the amounts of introduced NO_2 and O_3 did not produce significant differences in NO_2 concentrations across the different measurement channels. (Li et al., 2021). On this basis, O_3 interference is neglected for the present analysis.

3.3.3 Other interferences (nitro-aromatics, $ClNO_2$, N_2O_5)

Nitro-aromatics and nitrophenols can potentially generate NO_2 upon heating. To evaluate this potential interference in the ΣAN channel, we tested 3-nitrophenol and 1-nitropyrene (1 mg mL^{-1}; 1 µL injection) at 450 °C. The integrated NO_2 masses were below the detection limit, suggesting negligible interference for ΣANs under these test conditions.

Reactive nitrogen species such as $ClNO_2$ and N_2O_5 can thermally dissociate near the chosen TD temperatures (~450 °C and ~210 °C, respectively), which could bias gas-phase ΣANs and ΣPNs at night (Thaler et al., 2011; Sobanski et al., 2016). Because these species are largely nocturnal and photolyze rapidly after sunrise, daytime gas-phase ON retrievals are expected to be less affected (Li et al., 2021). In addition, particle-phase ONs are retrieved by differencing configurations that largely cancel common gas-phase contributions; therefore, pΣPNs and pΣANs are less sensitive to nocturnal gas-phase species under the present retrieval framework.

3.4 Precision and detection limits (Allan deviation)

Instrument precision was assessed using Allan deviation analysis with ultra-high-purity N_2 introduced to the inlet. The 1σ (1 s) NO_2 detection limits are 34 pptv (RT), 35 pptv (250 °C), and 33 pptv (450 °C), improving to 12–13 pptv at 10 s integration (Fig. 5). Propagating these channel precisions through the channel-differencing retrieval (Sect.

https://doi.org/10.5194/egusphere-2026-1574
Preprint. Discussion started: 24 March 2026

2.6) yields 1σ (1 s) detection limits of 49 pptv for gΣPNs, 49 pptv for pΣPNs, 48 pptv for gΣANs, and 68 pptv for pΣANs, consistent with values used for field reporting.

Table 2 compares detection limits reported for representative TD-based techniques. The present TD-CEAS achieves detection limits comparable to the lower end of reported TD methods, while providing simultaneous gas/particle partitioning using a single, compact NO_2 spectrometer framework.

4 Field deployment and example observations

4.1 Site description and ancillary measurements

The five-channel TD-CEAS was deployed on the rooftop (~15 m a.g.l.) of an office building at the Guangzhou Institute of Geochemistry (GIG), Guangzhou, China (113°21′49″ E, 23°8′46″ N). The site is located in a densely populated urban area influenced by nearby traffic corridors (~350 m). Two short intensive observation campaigns were conducted during 4-7 September 2025 and 1-2 October 2025 under clear, rain-free conditions.

Ancillary reactive nitrogen measurements were used to support evaluation of TD–CEAS performance and to enable post-processing correction of TD artifacts. NO was measured with a chemiluminescence NOx analyzer (Thermo Scientific 42i-TL). During the October deployment, PAN was measured concurrently by a GC–ECD system for intercomparison with the TD–CEAS gas-phase PN signal. Unless otherwise stated, times are reported in local time (UTC+8).

4.2 Measurement cycle, field configuration, and data processing

Ambient air was sampled through a $PM_{2.5}$ cyclone upstream of the inlet manifold. The instrument was operated in the five-channel configuration described in Sect. 2, with paired inlet/filter arrangements used to separate gas-only and total (gas + particle) signals. The gas-phase channels (RT-F, 250-F, 450-F) used an upstream particle filter

https://doi.org/10.5194/egusphere-2026-1574
Preprint. Discussion started: 24 March 2026

to remove particles prior to the TD reactors and CEAS, thereby providing NO_2, gΣPNs, and gΣANs by channel differencing. The particle-inclusive channels (250-UF, 450-UF) sampled air without upstream filtration so that both gas and particles entered the TD reactors, while a downstream filter removed particles immediately before the CEAS cavity. These channels therefore provided total (gas + particle) ΣPNs and ΣANs, and particle-phase quantities (pΣPNs and pΣANs) were obtained by differencing the total and gas-only channels.

Each channel was sampled for 1 min, after all five channels have been measured, a 1 min ultra-high-purity N_2 segment was introduced, yielding a 6-min measurement cycle. One-minute mean NO_2 values were calculated for each channel segment, and the derived ON products were reported at the 6 min cadence of the cycle. For clarity in time-series presentation, hourly means were calculated from the 6 min data (Sect. 4.3). Because thermally labile nocturnal species such as N_2O_5 and $ClNO_2$ can decompose in the TD inlets and bias gas-phase ON retrievals, the quantitative discussion in this work focuses on daytime gas-phase ONs, when such interferences are expected to be less important. Nighttime gas-phase ON data are shown for completeness and should be interpreted with caution. In contrast, particle-phase ONs were retained for both daytime and nighttime because the differencing approach largely cancels gas-phase interferences that are common to the gas-only and total configurations.

Laboratory-derived NO/NO_2 interferences in the ΣPN channels (Sect. 3.3.1) are expected to be most relevant under urban, high-NOx conditions. Accordingly, the correction model obtained from PAN-based laboratory experiments was applied to the 250 °C channel measurements using simultaneously measured NO from the chemiluminescence analyzer and NO_2 from the RT channel. The corrected 250 °C data

https://doi.org/10.5194/egusphere-2026-1574
Preprint. Discussion started: 24 March 2026

were then used to derive gΣPNs and pΣPNs. No additional correction was applied to ΣANs.

4.3 Time series and evaluation against PAN

Figure 6 shows hourly mean time series for NO, NO_2, gΣPNs, pΣPNs, gΣANs, and pΣANs during the two intensive observation periods. NO and NO_2 exhibited typical urban variability, with higher concentrations at night and lower concentrations during the day. The mean NO and NO_2 mixing ratios were 1.5 ± 2.1 ppbv and 14.8 ± 9.3 ppbv (mean ± 1σ) in September, and 1.4 ± 1.3 ppbv and 18.2±14.4 ppbv in October.

Daytime gΣPNs are elevated in both campaigns, with mean values of 2.8 ± 1.2 ppbv in September and 2.1 ± 1.2 ppbv in October and corresponding maxima of 8.4 and 5.8 ppbv, respectively. Particle-phase ΣPNs were smaller (e.g., 1.1 ± 0.5 ppbv in September) and showed less distinct diel structure. gΣANs displayed clear daytime maxima, with a mean of 1.0 ± 0.5 ppbv and 1.2 ± 0.5 ppbv in September and October, respectively. In contrast, pΣANs (1.0 ± 0.4 ppbv in September; 0.9 ± 0.5 ppbv in October) tended to peak at night, consistent with enhanced nighttime nitrate chemistry contributions and the expected nocturnal partitioning/production of low-volatility ONs (Fry et al., 2013).

During the October campaign, corrected gΣPNs were evaluated against independently measured PAN from the GC-ECD system. The two measurements agreed well in temporal variability, and linear regression yielded R^2 = 0.83. The regression slope indicates that PAN accounted for approximately 78% of daytime gΣPNs (Figs. S5–S6). This comparison supports the quantitative performance of the TD–CEAS gas-phase ΣPNs retrieval under urban conditions and provides an observational constraint on the extent to which PAN dominated the measured gΣPNs pool during the deployment.

https://doi.org/10.5194/egusphere-2026-1574
Preprint. Discussion started: 24 March 2026

These field observations demonstrate the capability of the five-channel TD–CEAS to provide continuous measurements of NO_2 and operational ON classes in both gas and particle phases at a 6 min cadence, with performance evaluation supported by independent PAN measurements and correction for NO/NO_2-dependent artifacts relevant to high-NOx environments.

5 Conclusions and outlook

We developed and characterized a five-channel TD-CEAS system for in situ measurements of NO_2 and operationally defined ON classes in both the gas and particle phases. The instrument couples a single NO_2 detector (405 nm) with two thermal dissociation setpoints (250 °C and 450 °C) and paired inlet/outlet configurations (upstream filtration for gas-only; downstream filtration for particle-inclusive sampling) to enable retrieval of gas- and particle-phase ΣPNs and ΣANs by channel differencing. In the field configuration used here, the system cycles through the five channels plus an N_2 reference segment, providing a complete set of NO_2, g/p ΣPNs, and g/p ΣANs at a 6 min cadence.

Laboratory characterization supported the selection of operational TD temperatures, with PAN (proxy for ΣPNs) exhibiting near-complete conversion at 250 °C and alkyl nitrate standards (proxies for ΣANs) reaching stable conversion at 450 °C for the residence time and reactor geometry employed. Under these conditions, particulate inorganic nitrate showed minimal contribution to the NO_2 signal at 450 °C. Allan deviation analysis yielded 1 σ (1 s) detection limits of 49 pptv for gΣPNs, 49 pptv for pΣPNs, 48 pptv for gΣANs, and 68 pptv for pΣANs. The gas-phase ΣPN response was validated using PAN, with TD–CEAS PAN-equivalent mixing ratios agreeing with GC–ECD measurements (slope = 0.987; R^2 = 0.988). For particle-phase ΣANs, an

https://doi.org/10.5194/egusphere-2026-1574
Preprint. Discussion started: 24 March 2026

operational calibration based on filter thermolysis of 2-EHN produced a linear response (slope = 1.036 ± 0.028) and a method detection limit of 0.029 μg NO_2. Dedicated interference experiments demonstrated that NO and NO_2 can introduce substantial, nonlinear biases in ΣPNs retrievals through radical chemistry in the TD inlet. These effects are reduced using a regression-based correction model that outperformed the reproduced lookup-table approach across the tested NOx conditions.

Field deployment at an urban site in Guangzhou during September–October 2025 demonstrated stable instrument operation under high-NOx conditions and produced continuous time series of gas- and particle-phase ON classes. During the October intensive period, corrected gΣPNs covaried well with independently measured PAN, with R^2 of 0.83, and PAN accounted for approximately 78% of daytime gΣPNs. The observed diel behavior, characterized by daytime enhancement of gas-phase ONs and nighttime enhancement of pΣANs, illustrates the utility of this approach for probing ON phase partitioning and reactive nitrogen processing in urban air. Because thermally labile nocturnal species such as N_2O_5 and $ClNO_2$ may interfere with gas-phase ON retrievals, nighttime gas-phase data should be interpreted cautiously and are not used here for quantitative discussion.

Future work should focus on strengthening traceability and expanding applicability of the method, including potential gas–particle separation artifacts, calibration representativeness, interference generalization with the goal of enabling reliable gas-phase ON detection across environments with reproducible processing. Overall, the five-channel TD–CEAS provides a practical measurement framework for continuous, class-resolved monitoring of organic nitrates in both phases, while explicitly addressing key challenges, particularly NO/NO_2-dependent TD chemistry, in high-NOx environments.

https://doi.org/10.5194/egusphere-2026-1574
Preprint. Discussion started: 24 March 2026

Data availability

Data are available upon request from the corresponding author (wangxm@gig.ac.cn).

Author contributions

XW acquired funds. XT designed and characterized the instrument with the support of XW and WS. XT carried out the instrument assessments. XT, HL, XY, and WS carried out the ONs measurements in the field. XT prepared the manuscript. XW and WS supervised the study. XW revised and edited the manuscript.

Competing interests

The authors declare that they have no conflict of interest.

Acknowledgements

This study was supported by the Ministry of Science and Technology of China (Grant No. 2022YFC3701103), National Natural Science Foundation of China (Grant No. 42321003), and the Department of Science and Technology of Guangdong (Grant Nos. 2023B0303000007 and 2023B1212060049).

https://doi.org/10.5194/egusphere-2026-1574
Preprint. Discussion started: 24 March 2026

References

Atkinson, R.: Atmospheric chemistry of VOCs and NOx, Atmos. Environ., 34, 2063–2101, https://doi.org/10.1016/s1352-2310(99)00460-4, 2000.

Chen, J., Wu, H., Liu, A. W., Hu, S. M., and Zhang, J.: Field measurement of NO_2 and RNO_2 by two-channel thermal dissociation cavity ring down spectrometer, Chin. J. Chem. Phys., 30, 493–498, https://doi.org/10.1063/1674-0068/30/cjcp1705084, 2017.

Chen, J., Wang, X., Zhang, J., Li, M., Liu, Z., Bi, Y., Wu, D., Yin, X., Gu, R., Jiang, Y., Shan, Y., Zhao, Y., Xue, L., and Wang, W.: Particulate organic nitrates at Mount Tai in winter and spring: Variation characteristics and effects of mountain-valley breezes and elevated emission sources, Environ. Res., 212, 113182, https://doi.org/10.1016/j.envres.2022.113182, 2022.

Day, D. A., Wooldridge, P. J., Dillon, M. B., Thornton, J. A., and Cohen, R. C.: A thermal dissociation laser-induced fluorescence instrument for in situ detection of NO_2, peroxy nitrates, alkyl nitrates, and HNO_3, J. Geophys. Res.-Atmos., 107, ACH 4-1–ACH 4-14, https://doi.org/10.1029/2001jd000779, 2002.

Fry, J. L., Draper, D. C., Zarzana, K. J., Campuzano-Jost, P., Day, D. A., Jimenez, J. L., Brown, S. S., Cohen, R. C., Kaser, L., Hansel, A., Cappellin, L., Karl, T., Hodzic Roux, A., Turnipseed, A., Cantrell, C., Lefer, B. L., and Grossberg, N.: Observations of gas- and aerosol-phase organic nitrates at BEACHON-RoMBAS 2011, Atmos. Chem. Phys., 13, 8585–8605, https://doi.org/10.5194/acp-13-8585-2013, 2013.

Fuchs, H., Dube, W. P., Cicioira, S. J., and Brown, S. S.: Determination of inlet transmission and conversion efficiencies for in situ measurements of the nocturnal nitrogen oxides, NO_3, N_2O_5 and NO_2, via pulsed cavity ring-down spectroscopy, Anal. Chem., 80, 6010–6017, https://doi.org/10.1021/ac8007253, 2008.

He, X. W., Zhang, C. L., Liu, P. F., Zhang, G., Wu, H., Peng, Y. X., Liu, J. F., Liu, C. T., and Mu, Y. J.: A novel photochemical conversion technique for reliable calibration of peroxyacetyl nitrate (PAN) analyzers, Sci. Total Environ., 872, 162164, https://doi.org/10.1016/j.scitotenv.2023.162164, 2023.

Keehan, N. I., Brownwood, B., Marsavin, A., Day, D. A., and Fry, J. L.: A thermal-dissociation-cavity ring-down spectrometer (TD-CRDS) for the detection of organic nitrates in gas and particle phases, Atmos. Meas. Tech., 13, 6255–6269, https://doi.org/10.5194/amt-13-6255-2020, 2020.

Kirchner, F., Mayer-Figge, A., Zabel, F., and Becker, K. H.: Thermal stability of peroxynitrates, Int. J. Chem. Kinet., 31, 127–144, https://doi.org/10.1002/(SICI)1097-4601(1999)31:2<127::AID-KIN6>3.0.CO;2-L, 1999.

Li, C. M., Wang, H. C., Chen, X. R., Zhai, T. Y., Chen, S. Y., Li, X., Zeng, L. M., and Lu, K. D.: Thermal dissociation cavity-enhanced absorption spectrometer for measuring NO_2, RO_2NO_2, and $RONO_2$ in the atmosphere, Atmos. Meas. Tech., 14, 4033–4051, https://doi.org/10.5194/amt-14-4033-2021, 2021.

Lin, C., Hu, R., Xie, P., Zhang, G., Liu, X., Tong, J., and Liu, W.: A three-channel thermal dissociation cavity ring-down spectrometer for simultaneous measurement of ambient total peroxy nitrates, total alkyl nitrates, and NO_2, Talanta, 270, 125524, https://doi.org/10.1016/j.talanta.2023.125524, 2024.

Lin, C., Hu, R., Liu, X., Ren, Y., Zhang, G., Tong, J., Wang, R., Wei, L., Xie, P., and Liu, W.: A high-sensitive multi-pass thermal dissociation cavity ring-down spectrometer for PNs and ANs measurement: Accurate quantification in realtime

https://doi.org/10.5194/egusphere-2026-1574
Preprint. Discussion started: 24 March 2026

under gas and particle phase, Sens. Actuators, B, 449, https://doi.org/10.1016/j.snb.2025.139090, 2026.

Murphy, J. G., Thornton, J. A., Wooldridge, P. J., Day, D. A., Rosen, R. S., Cantrell, C., Shetter, R. E., Lefer, B., and Cohen, R. C.: Measurements of the sum of HO_2NO_2 and $CH_3O_2NO_2$ in the remote troposphere, Atmos. Chem. Phys., 4, 377–384, https://doi.org/10.5194/acp-4-377-2004, 2004.

Neu, J. L., Lawler, M. J., Prather, M. J., and Saltzman, E. S.: Oceanic alkyl nitrates as a natural source of tropospheric ozone, Geophys. Res. Lett., 35, L13814, https://doi.org/10.1029/2008gl034189, 2008.

Paul, D., Furgeson, A., and Osthoff, H. D.: Measurements of total peroxy and alkyl nitrate abundances in laboratory-generated gas samples by thermal dissociation cavity ring-down spectroscopy, Rev. Sci. Instrum., 80, 114101, https://doi.org/10.1063/1.3258204, 2009.

Perring, A. E., Pusede, S. E., and Cohen, R. C.: An observational perspective on the atmospheric impacts of alkyl and multifunctional nitrates on ozone and secondary organic aerosol, Chem. Rev., 113, 5848–5870, https://doi.org/10.1021/cr300520x, 2013.

Roberts, J. M.: The atmospheric chemistry of organic nitrates, Atmos. Environ. A, 24, 243–287, https://doi.org/10.1016/0960-1686(90)90108-y, 1990.

Rollins, A. W., Smith, J. D., Wilson, K. R., and Cohen, R. C.: Real time in situ detection of organic nitrates in atmospheric aerosols, Environ. Sci. Technol., 44, 5540-5545, https://doi.org/10.1021/es100926x, 2010.

Rollins, A. W., Browne, E. C., Min, K. E., Pusede, S. E., Wooldridge, P. J., Gentner, D. R., Goldstein, A. H., Liu, S., Day, D. A., Russell, L. M., and Cohen, R. C.: Evidence for NOx control over nighttime SOA formation, Science, 337, 1210–1212, https://doi.org/10.1126/science.1221520, 2012.

Sadanaga, Y., Takaji, R., Ishiyama, A., Nakajima, K., Matsuki, A., and Bandow, H.: Thermal dissociation cavity attenuated phase shift spectroscopy for continuous measurement of total peroxy and organic nitrates in the clean atmosphere, Rev. Sci. Instrum., 87, 074102, https://doi.org/10.1063/1.4958167, 2016.

Sobanski, N., Schuladen, J., Schuster, G., Lelieveld, J., and Crowley, J. N.: A five-channel cavity ring-down spectrometer for the detection of NO_2, NO_3, N_2O_5, total peroxy nitrates and total alkyl nitrates, Atmos. Meas. Tech., 9, 5103–5118, https://doi.org/10.5194/amt-9-5103-2016, 2016.

Thaler, R. D., Mielke, L. H., and Osthoff, H. D.: Quantification of nitryl chloride at part per trillion mixing ratios by thermal dissociation cavity ring-down spectroscopy, Anal. Chem., 83, 2761–2766, https://doi.org/10.1021/ac200055z, 2011.

Thieser, J., Schuster, G., Schuladen, J., Phillips, G. J., Reiffs, A., Parchatka, U., Pohler, D., Lelieveld, J., and Crowley, J. N.: A two-channel thermal dissociation cavity ring-down spectrometer for the detection of ambient NO_2, RO_2NO_2 and $RONO_2$, Atmos. Meas. Tech., 9, 553–576, https://doi.org/10.5194/amt-9-553-2016, 2016.

Wooldridge, P. J., Perring, A. E., Bertram, T. H., Flocke, F. M., Roberts, J. M., Singh, H. B., Huey, L. G., Thornton, J. A., Wolfe, G. M., Murphy, J. G., Fry, J. L., Rollins, A. W., LaFranchi, B. W., and Cohen, R. C.: Total Peroxy Nitrates (Sigma PNs) in the atmosphere: the Thermal Dissociation-Laser Induced Fluorescence (TD-LIF) technique and comparisons to speciated PAN measurements, Atmos. Meas. Tech., 3, 593–607, https://doi.org/10.5194/amt-3-593-2010, 2010.

Wüst, L., Dewald, P., Türk, G., Lelieveld, J., and Crowley, J. N.: Influence of ambient NO and NO_2 on the quantification of total peroxy nitrates (ΣPNs) and total alkyl

https://doi.org/10.5194/egusphere-2026-1574
Preprint. Discussion started: 24 March 2026

nitrates (ΣANs) by thermal dissociation cavity ring-down spectroscopy (TD-CRDS), Atmos. Meas. Tech., 18, 1943–1959, https://doi.org/10.5194/amt-18-1943-2025, 2025.

Yu, K. Y., Zhu, Q., Du, K., and Huang, X. F.: Characterization of nighttime formation of particulate organic nitrates based on high-resolution aerosol mass spectrometry in an urban atmosphere in China, Atmos. Chem. Phys., 19, 5235–5249, https://doi.org/10.5194/acp-19-5235-2019, 2019.

Yu, X., Li, A. F., Ge, Y., Li, Y. M., Liao, K. Z., Huang, X. H., Li, J. J., and Yu, J. Z.: Simultaneous determination of aerosol inorganic and organic nitrogen by thermal evolution and chemiluminescence detection, Environ. Sci. Technol., 55, 11579–11589, https://doi.org/10.1021/acs.est.1c04876, 2021.

Zhang, G., Mu, Y., Liu, J., and Mellouki, A.: Direct and simultaneous determination of trace-level carbon tetrachloride, peroxyacetyl nitrate, and peroxypropionyl nitrate using gas chromatography-electron capture detection, J. Chromatogr. A, 1266, 110–115, https://doi.org/10.1016/j.chroma.2012.09.092, 2012.

Zhang, G., Mu, Y. J., Zhou, L. X., Zhang, C. L., Zhang, Y. Y., Liu, J. F., Fang, S. X., and Yao, B.: Summertime distributions of peroxyacetyl nitrate (PAN) and peroxypropionyl nitrate (PPN) in Beijing: Understanding the sources and major sink of PAN, Atmos. Environ., 103, 289–296, https://doi.org/10.1016/j.atmosenv.2014.12.035, 2015.

Zheng, W., Flocke, F. M., Tyndall, G. S., Swanson, A., Orlando, J. J., Roberts, J. M., Huey, L. G., and Tanner, D. J.: Characterization of a thermal decomposition chemical ionization mass spectrometer for the measurement of peroxy acyl nitrates (PANs) in the atmosphere, Atmos. Chem. Phys., 11, 6529–6547, https://doi.org/10.5194/acp-11-6529-2011, 2011.

Zhou, J., Zhao, W., Zhang, Y., Fang, B., Cheng, F., Xu, X., Ni, S., Zhang, W., Ye, C., Chen, W., and Venables, D. S.: Amplitude-modulated cavity-enhanced absorption spectroscopy with phase-sensitive detection: A new approach applied to the fast and sensitive detection of NO_2, Anal. Chem., 94, 3368–3375, https://doi.org/10.1021/acs.analchem.1c05484, 2022.

https://doi.org/10.5194/egusphere-2026-1574
Preprint. Discussion started: 24 March 2026

669 **Table 1.** Channel definitions and the corresponding quantities measured as NO_2 mixing
670 ratios by CEAS.

Channel	TD setpoint	Filter placement	What enters TD	CEAS measures
RT-F	RT	upstream	gas only	NO_2
250-F	250 °C	upstream	gas only	NO_2 + gΣPNs → NO_2
450-F	450 °C	upstream	gas only	NO_2 + gΣPNs + gΣANs → NO_2
250-UF	250 °C	downstream	gas + particles	NO_2 + (g+p)ΣPNs → NO_2
450-UF	450 °C	downstream	gas + particles	NO_2 + (g+p)ΣPNs + (g+p)ΣANs → NO_2

671

https://doi.org/10.5194/egusphere-2026-1574
Preprint. Discussion started: 24 March 2026

672 **Table 2.** Summary of reported 1σ detection limits (pptv) for thermal-dissociation-based
673 measurements of gΣPNs, pΣPNs, gΣANs and pΣANs from the literature and this study,
674 with the integration time (s) indicated in parentheses. For this study, ΣPN and ΣAN
675 detection limits are obtained by propagating Allan-deviation-derived NO_2 precision
676 through the channel-differencing retrieval. Reported detection limits as given in the
677 cited studies. "/" indicates not reported.

Reference	Instrument	Detection limit (pptv)			
		gΣPNs	gΣANs	pΣPNs	pΣANs
(Day et al., 2002)	TD-LIF	90 (10s)	90 (10s)	/	/
(Paul et al., 2009)	TD-CRDS	/	100 (1s)	/	/
(Rollins et al., 2010)	TD-LIF			/	45 (60s)
(Sobanski et al., 2016)	TD-CRDS	47 (1s)	40 (1s)	/	/
(Sadanaga et al., 2016)	TD-CAPS	7 (120s)	/	/	/
(Thieser et al., 2016)	TD-CRDS	28 (1s)	28 (1s)	/	/
(Chen et al., 2017)	TD-CRDS	/	100 (1s, RNO_2)	/	/
(Keehan et al., 2020)	TD-CRDS	220	220	/	/
(Li et al., 2021)	TD-CEAS	90 (6s)	90 (6s)	/	/
(Lin et al., 2024)	TD-CRDS	20.5 (1s)	18.3 (1s)	/	/
(Lin et al., 2026)	TD-CRDS	5.5 (30s)	6.2 (30s)	5.5 (30s)	6.2 (30s)
This study	TD-CEAS	49 (1s)	48 (1s)	49 (1s)	68 (1s)

678

https://doi.org/10.5194/egusphere-2026-1574
Preprint. Discussion started: 24 March 2026

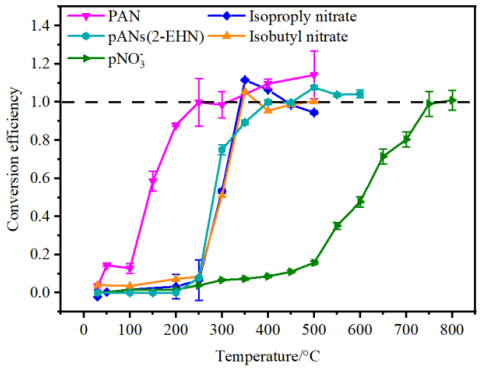

679

680 **Figure 1.** Temperature-dependent thermal dissociation response ("thermal spectrum")
681 for representative organic nitrate standards and aerosol nitrate in the TD inlet. Shown
682 are peroxyacetyl nitrate (PAN; proxy for ΣPNs), isopropyl nitrate and isobutyl nitrate
683 (proxies for gas-phase ΣANs), particulate 2-ethylhexyl nitrate (2-EHN; proxy for
684 particle-phase organic nitrates), and particulate inorganic nitrate (pNO_3^-, generated
685 from $NaNO_3$ aerosol). The conversion efficiency (unitless) is calculated as the NO_2
686 yield at each setpoint normalized to the high-temperature plateau for each compound;
687 the dashed line denotes unity (complete conversion). Error bars indicate ±1σ from
688 replicate measurements. Temperature refers to the TD tube wall temperature at the
689 thermocouple location.

690

https://doi.org/10.5194/egusphere-2026-1574
Preprint. Discussion started: 24 March 2026

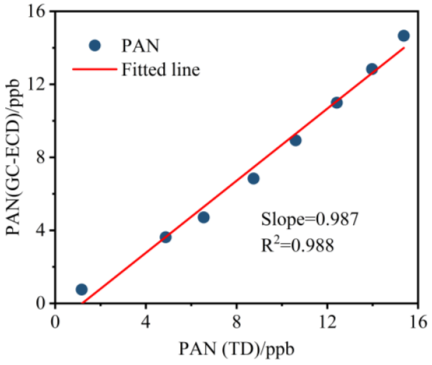

691

692 **Figure 2.** Cross-validation of PAN measured TD-CEAS against an independent gas
693 chromatography–electron capture detector (GC–ECD) measurement. PAN (TD) is
694 derived from the TD–CEAS 250 °C channel after subtraction of the room-temperature
695 NO_2 channel. The red line shows a least-squares linear regression; the slope and
696 coefficient of determination (R^2) are reported in the panel.

697

https://doi.org/10.5194/egusphere-2026-1574
Preprint. Discussion started: 24 March 2026

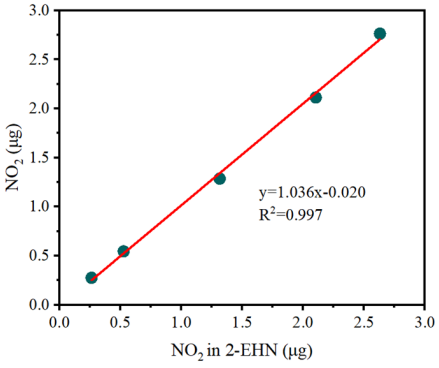

698

699 **Figure 3.** Calibration of particulate ΣAN response using filter thermolysis of
700 2-ethylhexyl nitrate (2-EHN). The recovered NO_2 mass (integrated CEAS signal) is
701 plotted as a function of the expected NO_2 mass associated with the injected 2-EHN
702 amount. The red line denotes a linear regression; the fit equation and R^2 are given in
703 the panel.

704

https://doi.org/10.5194/egusphere-2026-1574
Preprint. Discussion started: 24 March 2026

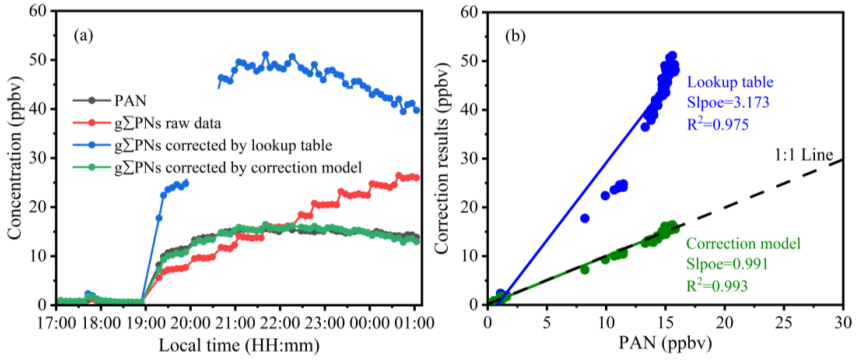

Figure 4. (a) The measured PAN and gΣPNs alongside the correction PNs by lookup table and correction model, (b) Linear fit of correction results of lookup table and correction model with measured PAN. PAN is measured by GC-ECD, and gΣPNs is measured by TD-CEAS through the difference subtraction method.

https://doi.org/10.5194/egusphere-2026-1574
Preprint. Discussion started: 24 March 2026

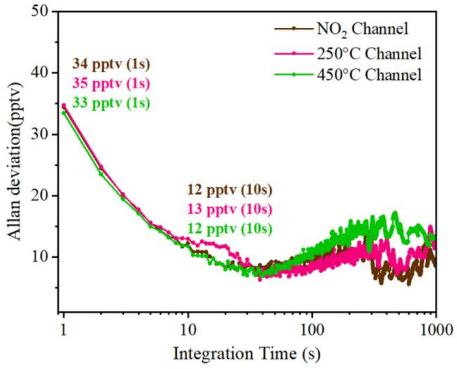

711

712 **Figure 5.** Allan Deviation of NO_2 mixing ratios retrieved by CEAS for the room-
713 temperature NO_2 channel and the heated TD channels (250 °C and 450 °C), calculated
714 from continuous ultra-high-purity N_2 sampling. The Allan deviation quantifies 1σ
715 precision as a function of integration time; annotated values indicate the 1 s and 10 s
716 precisions for each channel.

717

https://doi.org/10.5194/egusphere-2026-1574
Preprint. Discussion started: 24 March 2026

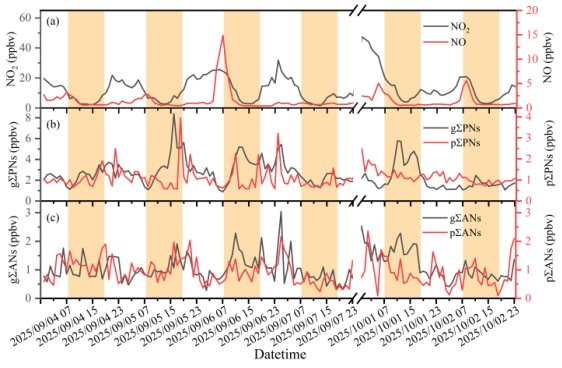

Figure 6. Hourly mean time series of NO measured by a Thermo Scientific 42i-TL analyzer, NO_2 measured by the RT channel, and class-resolved organic nitrates measured by the five-channel TD–CEAS during two intensive periods at the urban Guangzhou site (4–7 September 2025 and 1–2 October 2025; local time, UTC+8). From top to bottom, panels show NO and NO_2, gas- and particle-phase peroxy nitrates (gΣPNs and pΣPNs), and gas- and particle-phase alkyl nitrates (gΣANs and pΣANs). ΣPNs are shown after application of the NO/NO_2-dependent correction model derived from laboratory PAN experiments. Orange shading indicates daytime. All mixing ratios are in ppbv.